Materials Research Proceedings 39 (2024) 17-24 https://doi.org/10.21741/9781644903094-3

Thermal Conductivity of Steel-Steel Composite Metal Foam through Computational Modeling

Zubin Chacko [1] and Afsaneh Rabiei [1,a *]

[1] Advanced Materials Research Laboratory (AMRL), Department of Mechanical and Aerospace Engineering, North Carolina State University, Raleigh, NC, 27606, USA

[a] arabiei@ncsu.edu

Keywords: Composite Metal Foams, Effective Thermal Diffusivity, Effective Thermal Conductivity, Computational Modeling, ANSYS Fluent, Thermal Insulation

Abstract. Thermal capabilities of Steel-Steel composite metal foam (CMF) against extremely high temperatures using computational methods have been investigated and contrasted with the characteristics of the base bulk steel materials. A physics-based three-dimensional model of CMF was constructed using Finite Element Analysis software for analyzing its thermal conductivity. The model built and analyzed in ANSYS Fluent was based on high temperature guarded-comparative longitudinal heat flow technique. ANSYS Fluent allows for the inclusion of air in the model, which is the main contributor to the low thermal conductivity of CMF compared to its constituent material. The model's viability was checked by comparing the computational and experimental results, which indicated approximately 2% deviation throughout the investigated temperature range. Excellent agreement between the experimental and computational model results shows that the CMF can be first modeled and analyzed using the proposed computational technique for the desired thermal insulation application before manufacturing. Based on the ratios of the matrix to the spheres and the thickness of the sphere walls, CMF can be tailored to the density requirements and then checked for its thermal performance using the model, thereby lowering the cost involved in its manufacturing and thermal characterization experiments.

Introduction

A type of metal foam called composite metal foam (CMF) is created using hollow metal spheres encased in a metallic matrix. The cell walls and the general integrity of the structure are strengthened by the metal matrix, which surrounds and fills the spaces between a loosely packed, random arrangement of hollow metal spheres. Casting [1] or powder metallurgy (PM) [2] are two methods used to make CMFs. Metal foams are renowned for being efficient and effective heat sinks due to the substantial surface area that the porosities in these materials provide [3]. A prior work [4] reported the specific heat capacity, effective thermal conductivity, and coefficient of thermal expansion of CMFs. However, it is crucial to note that only the temperature range between 300 and 600 ºC was used to study the thermal conductivity values of S-S CMF. Identifying the fundamental thermal characteristics of S-S CMF at even higher temperatures, close to 1000 ºC, is crucial for its application in the industry. CMF characteristics have been shown to vary with stainless steel spherical size and wall thickness and can be tailored for specific uses [5]. Therefore, it would be advantageous if crucial thermal characteristics, like the thermal conductivity of S-S CMF, could be anticipated using commercial modeling software. To develop the best S-S CMF for the intended application, sphere size, and wall thickness can be changed in computational solvers. Results can then be verified experimentally, thereby reducing the cost of testing.

This study uses a computational method to investigate the thermal conductivity of S-S CMF from ambient temperature to 1000 °C. First, to forecast the thermal conductivity of Composite metal foams with 2 mm steel hollow spheres and 316L stainless steel matrix [(2 mm sphere) S-S CMF] from 100 to 1000 °C, a physics-based three-dimensional model was created utilizing the

Materials Research Proceedings 39 (2024) 17-24 https://doi.org/10.21741/9781644903094-3

high-temperature guarded-comparative longitudinal heat flow (GCH) technique. The results of the thermal conductivity data obtained through computational modeling were compared with experimental data to determine the model's viability.

Computational modeling

Model Description. First, the (2 mm sphere) S-S CMF is modeled based on the experimental sample used in the earlier work [4]. Spherical porosities were added and organized in a body-centered cubic (BCC) structure with inner diameters of 1.8 mm to mimic the geometry of the CMF with 2 mm stainless steel hollow spheres and 100 µm wall thickness. These porosities represent the amount of air inside the hollow stainless-steel spheres. Spacing was added between the porosities to represent the spherical wall thickness and achieve the average overall packing efficiency of S-S CMF, defined as 59% [2]. The sphere walls and matrix are assumed to be a single entity in the model to reduce the complexity of the model and speed up calculations. Finally, the matrix of the CMF has been regarded as a bulk material. Fig. 1(a) depicts the model of the CMF with the porosity configuration.

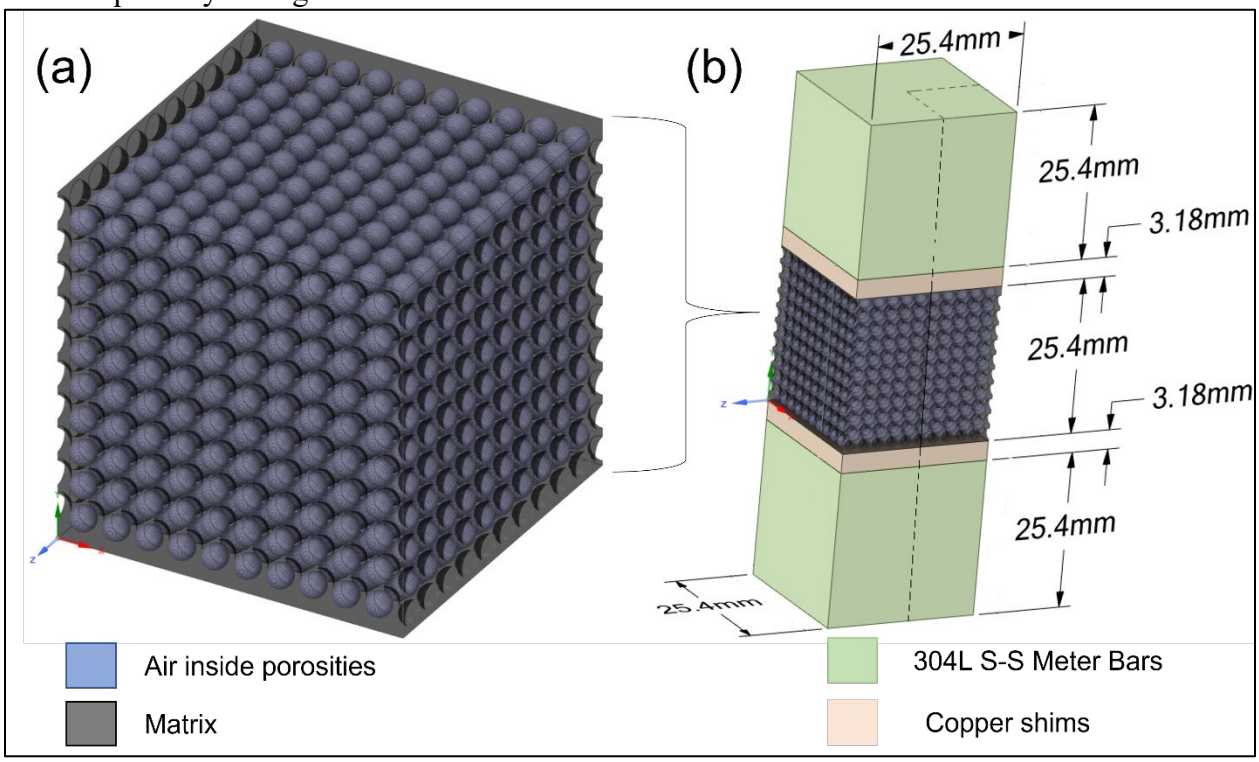

Fig. 1 S-S CMF model for thermal conductivity measurements using the GCH technique.

Fig. 1(b) depicts the computational model based on the GCH approach. Meter bars (304 L stainless steel), copper shims (copper), matrix and hollow spheres (316 L stainless steel), and air (within matrix and porosities) are the model's key constituents. The geometrical parameters shown in Fig. 1(b) are taken from the earlier work [4]. These components' thermal properties for the model can be found in Tables 1,2 and 3. Due to symmetry and unidirectional heat flow, only a quarter of the experimental setup was used as a representative volume for computational needs. Fig. 2 depicts the computational domain under consideration. The considered domain still represents bulk S-S CMF and is large enough to accommodate multiple spheres (5 across direction of heat flow and 11 in the direction of heat flow) in the body. The ANSYS Workbench's integrated meshing module was then used to mesh the derived geometric model. Within the problem domain, hexahedral elements were used to construct an organized grid.

Table 1. Thermal properties of the 316L and 304L steels at various temperature [6].

Temperature (ºC)	316 L Stainless Steel			304 L Stainless Steel	
	Specific Heat (J kg^{-1} K^{-1})	Thermal Conductivity (W m^{-1} K^{-1})	Thermal Diffusivity (mm^2 s^{-1})	Specific Heat (J kg^{-1} K^{-1})	Thermal Conductivity (W m^{-1} K^{-1})
25	498.58	13.93	3.52	509.64	12.94
200	521.82	16.68	4.05	533.23	15.77
400	548.38	19.82	4.63	560.19	19.01
600	574.94	22.97	5.19	587.15	22.24
800	601.50	26.11	5.72	614.11	25.48
1000	628.06	29.25	6.23	641.08	28.72

Table 2. Thermal properties of copper at various temperature [7], [8].

Temperature (ºC)	Specific Heat (J kg^{-1} K^{-1})	Thermal Conductivity (W m^{-1} K^{-1})
27	388.69	401
227	408.87	388
427	429.05	374
627	449.23	360
827	469.39	348
1027	489.57	338

Table 3. Thermal properties of air at various temperature [9].

Temperature (ºC)	Density (kg m^{-3})	Specific Heat (J kg^{-1} K^{-1})	Thermal Conductivity (W m^{-1} K^{-1})	Viscosity (x 10^{-5} kg m^{-1} s^{-1})
25	1.184	1007	0.02551	1.849
200	0.7459	1023	0.03779	2.577
400	0.5243	1069	0.05015	3.261
600	0.4042	1115	0.06093	3.846
800	0.3289	1153	0.07037	4.362
1000	0.2772	1184	0.07868	4.826

Assumptions and Boundary Conditions. The meshed model was loaded into the FLUENT module of the ANSYS WORKBENCH. Here, the experiment's boundary conditions were applied, the necessary temperature gradients were measured, and the thermal conductivities at various temperatures were calculated. Applied boundary conditions are depicted schematically in Fig. 2, resembling the GCH method.

As mentioned earlier, the matrix was considered a bulk material in the computational domain. However, the PM method's matrix processes have porosities resembling a closed-cell foam structure. An analytical model for closed-cell metal foams was used to establish the matrix's thermophysical parameters and then entered into ANSYS FLUENT to represent the matrix's porous nature. In this work, the Maxwell-Eucken equation [10] was utilized to determine the thermal conductivity of the matrix used in the model:

Materials Research Proceedings 39 (2024) 17-24 https://doi.org/10.21741/9781644903094-3

$$k_m = \frac{k_s f_s + k_a f_a \frac{3k_s}{2k_s + k_a}}{f_s + f_a \frac{3k_s}{2k_s + k_a}} \quad (1)$$

Here, k_m, k_s, and k_a are thermal conductivities ($Wm^{-1}\,{}^oK^{-1}$) of the solid bulk matrix, 316 L stainless steel, and air, respectively. Also, f_s and f_a are 316L stainless steel and air volume fractions within S-S CMF structure, respectively.

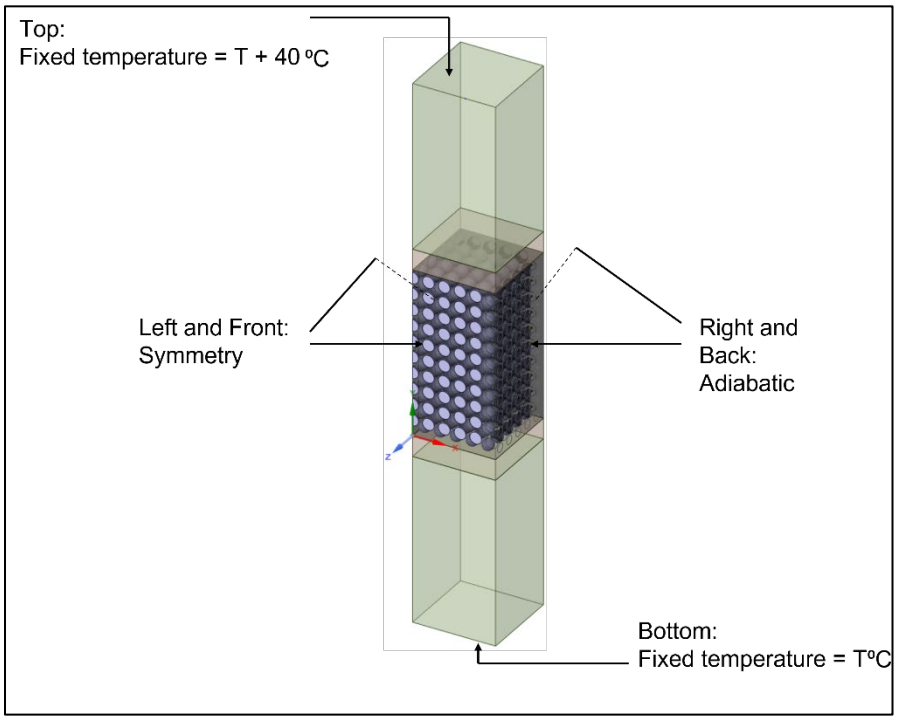

Fig. 2 Boundary conditions for the (2-mm sphere) S-S CMF as per the GCH experiments.

According to reports [11], metal foams have the same specific heat as their parent material; hence the specific heat of the matrix is equated to that of the solid 316L stainless steel.

Solution. ANSYS Fluent's steady-state condition solver was employed, and Fourier's Law was used to determine the thermal conductivity of the S-S CMF from 100 to 1000 °C.

Results and discussions

Fig. 3 shows the temperature-dependent thermal conductivity of S-S CMF as per the results from the computational model along with the data from the GCH approach used in the earlier work [4]. The experimental data and the computational model both demonstrate that the S-S CMF exhibits significantly lower thermal conductivity than its main constituent, 316L stainless steel. Air trapped inside the sample's porosities, which has a substantially lower thermal conductivity than solid 316L stainless steel, is the cause of the lower thermal conductivity in CMF.

Since spheres make up 59 volume percent of S-S CMF, the matrix makes up 41 percent of the volume. With a wall thickness to sphere outer diameter ratio of 1/20, the air occupies about 73% of each sphere's cavity. As such, the air content inside the spheres is predicted to be about 43% of the total volume of the S-S CMF sample. In addition, from the 41% matrix that makes up the structure of CMF, around 46% of it is air in its micro-porosities, accounting for roughly 19% of air in the matrix (depending on the compaction of the matrix powder). Intrinsically, the total air in S-S CMF samples is about 19%+43%=62%. Air content in the matrix's microporosities (produced by powder metallurgy) and the air trapped inside the cavities of spheres lowers the S-S CMF thermal conductivity.

Materials Research Proceedings 39 (2024) 17-24 https://doi.org/10.21741/9781644903094-3

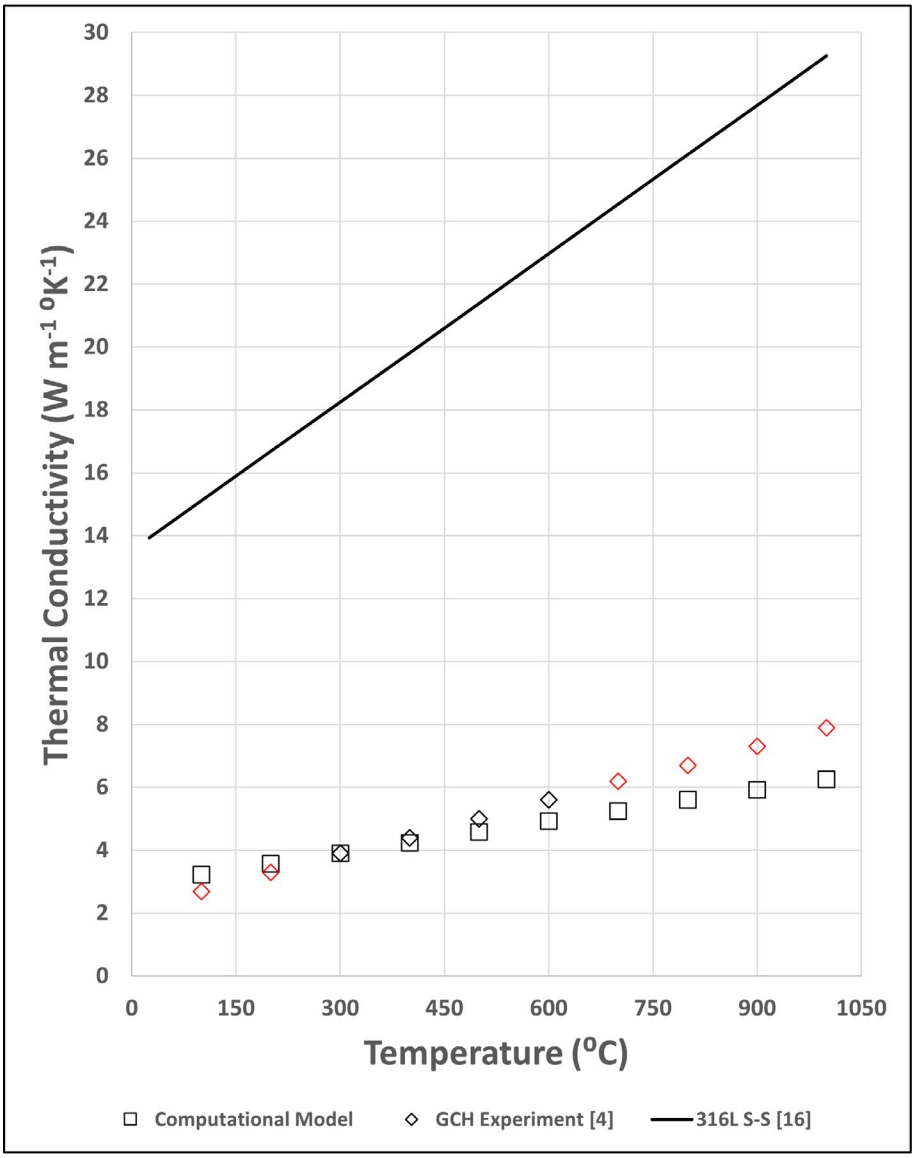

Fig. 3 Thermal conductivities of (2 mm sphere) S-S CMF by the computational model and the GCH experimental techniques. (Red data points are the extrapolated values from the GCH experiments).

Results also indicate differences in the thermal conductivity results between the experimental method used in the prior work [4] and the computational model—an average variance of 6% in the thermal conductivity readings between 300 and 600 ºC. The extrapolated thermal conductivity data from the GCH experiment reveals an average departure of 15% from the computer modeling values for temperatures beyond 600 ºC. Additionally, in contrast to the computational findings of the current work, we can see that the increase in thermal conductivity of S-S CMF with the temperature rise is more significant in the case of the GCH experimental technique [4]. Environmental factors, sample preparation, and measurement sensors may be to blame for the variations [12]. At high temperatures, convection, radiation, and non-unidirectional heat flow through the sample all contribute to increased measurement inaccuracy for the GCH technique [13]. For the GCH approach, extremely flat and parallel surfaces are necessary [12]. The air gaps between the sample surfaces and the hot and cold plates caused by roughness may significantly increase interfacial thermal resistance and a temperature drop. In the case of CMF, the contact surfaces are highly

porous (partial spheres and porous matrix); hence the air gaps can impact the thermal conductivity measurements.

The computational results were also compared with another experimental work [14] which employed the laser flash technique for finding the thermal conductivity of [(2 mm sphere) S-S CMF. It is well known that cellular materials' thermal conductivity is greatly influenced by their density [15]. Therefore, thermal conductivity results normalized by density are compared and shown in Fig. 4. The sample used for the computational studies was based on the GCH experimental work and hence was normalized by 2.7 g cm^{-3} [4], while the laser flash experiment samples had an average density of 2.6 g cm^{-3} [14]. Here we can see a close agreement between the computational results of this study with the experimental data of the laser flash experiments. Laser flash analysis is one of the most effective and adaptable ways to test thermal characteristics. Utilizing the appropriate sample holders and measurement settings determines thermal conductivity. The laser flash achieves High-accuracy temperature sensing using non-contact, non-destructive methods [16]. Hence it is devoid of the inaccuracies inherent in the GCH technique due to the high temperature and porous nature of CMF. Even though the computational model is based on the GCH technique, it avoids the environmental and sample contact surface effects by the applied ideal boundary conditions.

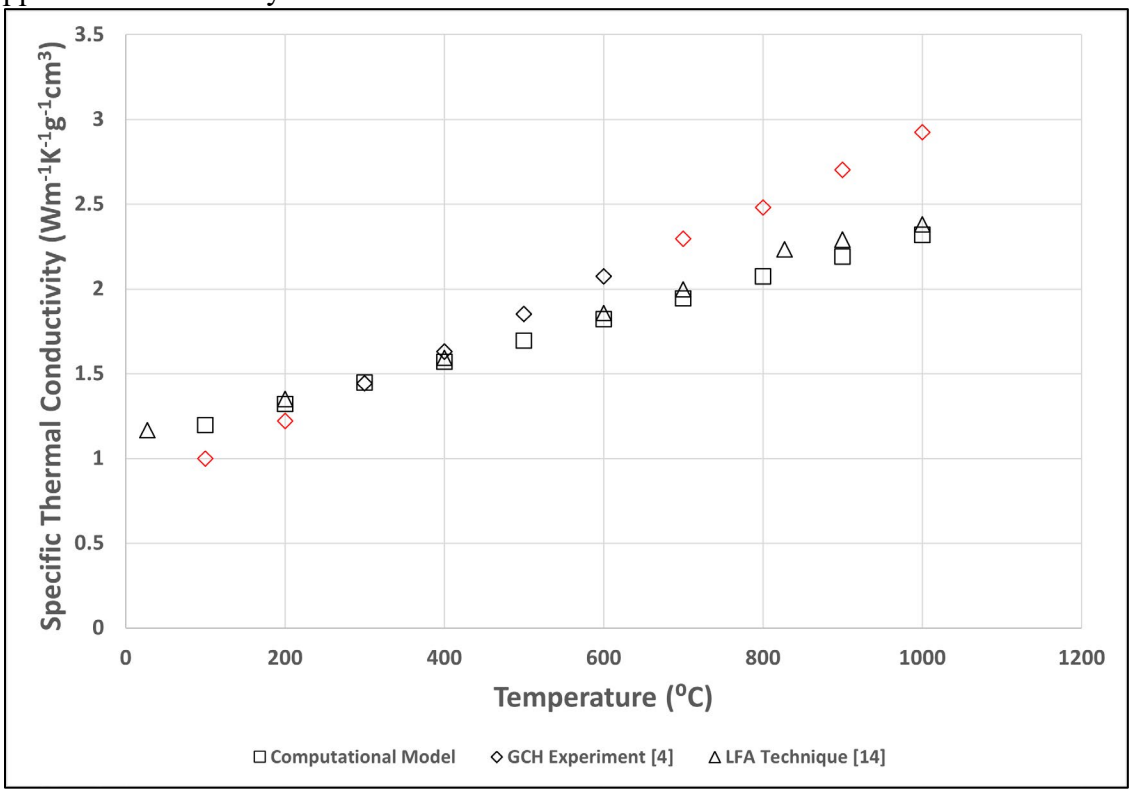

Fig. 4 Specific thermal conductivity of S-S CMF (Red data points are the extrapolated values from the GCH experiments).

We may therefore say that the computational model created here made fair assumptions and can successfully and reasonably predict the thermal conductivities of S-S CMF. The viability of S-S CMF for a specific thermal insulation application may be predicted very precisely using this model before it is produced. The model's sphere sizes and matrix porosity can be adjusted to estimate the thermal conductivity of different S-S CMF design iterations. This aids in choosing the best S-S CMF design for each application. As a result, the model can aid in reducing the cost of S-S CMF manufacture and experimental testing.

Conclusion

The following conclusions have been reached based on the findings of the experimental and modeling results:

- To forecast the thermal conductivity of S-S CMF, a straightforward physics-based computational model was created using ANSYS Fluent. The results of the computationally predicted thermal conductivity were compared with the earlier experiments and showed good agreement.
- It was shown that the S-S CMF's thermal conductivity is six times lower than that of its parent material, 316L S-S.
- The S-S CMF's porosities contain a high volume-fraction of air, which helps explain its low thermal conductivity.
- The S-S CMF thermal resistance can be altered by changing its porosity content in the matrix throughout adjusting the compaction pressure and by modifying the sphere-to-matrix ratios, and spheres geometry/characteristics.
- The cost of manufacturing and thermal experiments can be decreased by using the aforementioned computational model to help determine production parameters for S-S CMFs, such as the sphere sizes and porosity of the matrix.

Acknowledgment
This study is part of a project funded by the Department of Transportation (DOT) Pipeline and Hazardous Materials Safety Administration (PHMSA), project number PH957-20-0075.

References

[1] L. J. Vendra and A. Rabiei, "A study on aluminum–steel composite metal foam processed by casting," *Materials Science and Engineering: A*, vol. 465, no. 1–2, pp. 59–67, Sep. 2007. https://doi.org/10.1016/j.msea.2007.04.037

[2] B. P. Neville and A. Rabiei, "Composite metal foams processed through powder metallurgy," *Mater Des*, vol. 29, no. 2, 2008. https://doi.org/10.1016/j.matdes.2007.01.026

[3] W. H. Hsieh, J. Y. Wu, W. H. Shih, and W. C. Chiu, "Experimental investigation of heat-transfer characteristics of aluminum-foam heat sinks," *Int J Heat Mass Transf*, vol. 47, no. 23, pp. 5149–5157, Nov. 2004. https://doi.org/10.1016/j.ijheatmasstransfer.2004.04.037

[4] S. Chen, J. Marx, and A. Rabiei, "Experimental and computational studies on the thermal behavior and fire-retardant properties of composite metal foams," *International Journal of Thermal Sciences*, vol. 106, pp. 70–79, Aug. 2016. https://doi.org/10.1016/j.ijthermalsci.2016.03.005

[5] A. Rabiei and M. Garcia-Avila, "Effect of various parameters on properties of composite steel foams under variety of loading rates," *Materials Science and Engineering: A*, vol. 564, pp. 539–547, Mar. 2013. https://doi.org/10.1016/j.msea.2012.11.108

[6] C. S. Kim, "Thermophysical properties of stainless steels," 1975.

[7] B. Banerjee, An evaluation of plastic flow stress models for the simulation of high-temperature and high-strain-rate deformation of metals. 2005.

[8] J. G. Hust and A. B. Lankford, "Thermal conductivity of aluminum, copper, iron, and tungsten for temperatures from 1 K to the melting point," Jun. 1984.

[9] Y. A. Çengel, *Heat Transfer: A Practical Approach*. McGraw-Hill, 2003.

[10] A. Eucken, “Allgemeine Gesetzmäßigkeiten für das Wärmeleitvermögen verschiedener Stoffarten und Aggregatzustände,” *Forschung auf dem Gebiete des Ingenieurwesens*, vol. 11, no. 1, pp. 6–20, Jan. 1940. https://doi.org/10.1007/BF02584103

[11] M. F. Ashby, A. Evans, N. A. Fleck, L. J. Gibson, J. W. Hutchinson, and H. N. G. Wadley, "Metal foams: a design guide," *Mater Des*, vol. 23, no. 1, p. 119, Feb. 2002. https://doi.org/10.1016/S0261-3069(01)00049-8

[12] "Standard Test Method for Thermal Conductivity of Solids by Means of the Guarded-Comparative-Longitudinal Heat Flow Technique 1". https://doi.org/10.1520/E1225-04.

[13] X.-H. An, J.-H. Cheng, H.-Q. Yin, L.-D. Xie, and P. Zhang, "Thermal conductivity of high temperature fluoride molten salt determined by laser flash technique," *Int J Heat Mass Transf*, vol. 90, pp. 872–877, Nov. 2015. https://doi.org/10.1016/j.ijheatmasstransfer.2015.07.042

[14] A. Rabiei, N. Amoafo-Yeboah, E. Huseboe, and C. Scemama, "A Study on Thermal Properties of Composite Metal Foams for Applications in Tank Cars Carrying Hazardous Materials," in *Minerals, Metals and Materials Series*, 2022. doi: 10.1007/978-3-030-92567-3_23

[15] A. N. Abramenko, A. S. Kalinichenko, Y. Burtser, V. A. Kalinichenko, S. A. Tanaeva, and I. P. Vasilenko, "Determination of the thermal conductivity of foam aluminum," *Journal of Engineering Physics and Thermophysics*, vol. 72, no. 3, pp. 369–373, May 1999. https://doi.org/10.1007/BF02699196

[16] S. Min, J. Blumm, and A. Lindemann, "A new laser flash system for measurement of the thermophysical properties," *Thermochim Acta*, vol. 455, no. 1–2, pp. 46–49, Apr. 2007. https://doi.org/10.1016/j.tca.2006.11.026